

Particle Physics at the LHC - Seminar Report

Triple and Quartic Gauge Couplings

Gernot KNIPPEN

June 17, 2014

Physikalisches Institut
University of Freiburg



Abstract

This review summarizes the results of four important articles on multiple gauge couplings and future prospects on quartic gauge coupling measurements published in 2013 and 2014. All measurements were consistent with the Standard Model. Limits on triple gauge couplings improving or reaching similar precision to those obtained by LEP experiments were derived by using differential ZZ and WW cross sections, respectively. First direct constraints on quartic gauge couplings were calculated from the total $W^\pm W^\pm jj$ cross section. Future triboson production and vector boson scattering analyses might give further constraints on quartic gauge couplings.

1 Introduction

The production of vector boson pairs at the Large Hadron Collider (LHC) provides a great possibility for important tests of the electroweak sector of the Standard Model (SM) continuing, improving and enhancing the work done at the Tevatron and the LEP collider. A lot of effort is made to investigate multiple vector boson couplings: triple gauge couplings (TGC) and quartic gauge couplings (QGC).

In this article the latest results from the ATLAS experiment are presented. It is structured as follows: The second section gives a motivation for TGCs and QGCs arising from the SM and describes multiple coupling contributions in a model independent effective field theory approach following [1] and [2]. The third section summarizes the latest official results from the ATLAS experiment concerning anomalous neutral TGC [3]. The fourth section covers the results on charged TGC [4]. In section five this year's results from the ATLAS experiment showing evidence for electroweak $W^\pm W^\pm jj$ production and giving first direct constraints on QGC [5] are presented. Section six covers possible future results on QGC as presented in [6]. Conclusions are drawn in the last section.

2 Triple and Quartic Gauge Couplings Arising in the Standard Model and Beyond

To understand why TGCs and QGCs arise in the SM it is crucial to understand the electroweak interaction theory, unifying the fundamental forces of weak and electromagnetic interaction. In the following a short reminder of the SM's electroweak sector is given with special attention to gauge boson self coupling terms. The concept of "effective field theory" (EFT) together with TGC and QGC effective Lagrangians is described afterwards.

2.1 Triple and Quartic Gauge Couplings Arising in the Standard Model

The theory of quantum electrodynamics (QED) is invariant under local phase transformations ($U(1)$)

$$\psi \rightarrow \psi' = e^{iQ\alpha(x)}\psi, \quad (1)$$

where ψ is the fermion field, Q the charge and $\alpha(x)$ the local phase transformation angle. The La-

grangian of QED \mathcal{L}_{QED} is given by

$$\mathcal{L}_{QED} = \bar{\psi}(i\gamma^\mu\partial_\mu - m)\psi - Q\bar{\psi}\gamma^\mu\psi A_\mu - \frac{1}{4}F_{\mu\nu}F^{\mu\nu}, \quad (2)$$

where m is the fermion mass, A_μ the photon field and $F_{\mu\nu}$ the field strength tensor given by

$$F_{\mu\nu} = \partial_\mu A_\nu - \partial_\nu A_\mu. \quad (3)$$

The summands of the Lagrangian \mathcal{L}_{QED} can be interpreted as

- the free fermion propagation part \mathcal{L}_0 ,
- the fermion-photon interaction and
- the photon kinetic energy.

Unifying QED and the theory of weak interactions yields the theory of electroweak interactions. It is invariant under $SU(2)_L \otimes U(1)$

$$\psi \rightarrow \psi' = e^{\frac{i}{2}\vec{\tau}\vec{\alpha}(x)}e^{i\frac{Y}{2}\beta(x)}\psi \quad (4)$$

and its dynamics are described by the following Lagrangian \mathcal{L}_{EW} ¹:

$$\begin{aligned} \mathcal{L}_{EW} = & \bar{\chi}_L\gamma^\mu \left(i\partial_\mu - g\frac{\vec{\tau}}{2}\vec{W}_\mu - g'\frac{Y}{2}B_\mu \right) \chi_L \\ & + \bar{\psi}_R \left(i\partial_\mu - g'\frac{Y}{2}B_\mu \right) \psi_R + \mathcal{L}_{kin}. \end{aligned} \quad (5)$$

Here $\vec{\tau}$ is the weak isospin ($SU(2)$ generator), Y is the weak hypercharge, χ_L and ψ_R are the fermionic left- and right-handed part respectively and \vec{W}_μ and B_μ are the electroweak gauge fields. The gauge invariant term \mathcal{L}_{kin} describing the gauge field kinetics is given by

$$\mathcal{L}_{kin} = -\frac{1}{4}B_{\mu\nu}B^{\mu\nu} - \frac{1}{4}\vec{W}_{\mu\nu}\vec{W}^{\mu\nu}, \quad (6)$$

where the rank two tensors $B_{\mu\nu}$ and $\vec{W}_{\mu\nu}$ are defined in the following way

$$B_{\mu\nu} := \partial_\mu B_\nu - \partial_\nu B_\mu, \quad (7)$$

$$\vec{W}_{\mu\nu} := \partial_\mu\vec{W}_\nu - \partial_\nu\vec{W}_\mu + g\vec{W}_\mu \times \vec{W}_\nu. \quad (8)$$

The last summand in $\vec{W}_{\mu\nu}$ arises because of the non-abelian gauge structure. It is the reason for gauge boson self-interaction terms in the Lagrangian. Expanding \mathcal{L}_{kin} and changing to the observable mass eigenstate gauge fields ($W_\mu^{(\dagger)}$, Z_μ and A_μ) one gets the following cubic and quartic interaction terms be-

¹Only the Lagrangian before electroweak symmetry breaking is considered.

sides other in this recapitulation unimportant ones

$$\begin{aligned}
\mathcal{L}_3 = & -ie \cot \theta_W \left[(\partial^\mu W^\nu - \partial^\nu W^\mu) W_\mu^\dagger Z_\nu \right. \\
& - \left. (\partial^\mu W^{\nu\dagger} - \partial^\nu W^{\mu\dagger}) W_\mu Z_\nu \right. \\
& \left. + W_\mu W_\nu^\dagger (\partial^\mu Z^\nu - \partial^\nu Z^\mu) \right] \\
& - ie \left[(\partial^\mu W^\nu - \partial^\nu W^\mu) W_\mu^\dagger A_\nu \right. \\
& - \left. (\partial^\mu W^{\nu\dagger} - \partial^\nu W^{\mu\dagger}) W_\mu A_\nu \right. \\
& \left. + W_\mu W_\nu^\dagger (\partial^\mu A^\nu - \partial^\nu A^\mu) \right], \quad (9) \\
\mathcal{L}_4 = & -\frac{e^2}{2 \sin^2 \theta_W} \left[(W_\mu^\dagger W^\mu)^2 - W_\mu^\dagger W^{\mu\dagger} W_\nu W^\nu \right] \\
& - e^2 \cot^2 \theta_W \left[W_\mu^\dagger W^\mu Z_\nu Z^\nu - W_\mu^\dagger Z^\mu W_\nu Z^\nu \right] \\
& - e \cot \theta_W \left[2W_\mu^\dagger W^\mu Z_\nu A^\nu - W_\mu^\dagger Z^\mu W_\nu A^\nu \right. \\
& \left. - W_\mu^\dagger A^\mu W_\nu Z^\nu \right] \\
& - e^2 \left[W_\mu^\dagger W^\mu A_\nu A^\nu - W_\mu^\dagger A^\mu W_\nu A^\nu \right], \quad (10)
\end{aligned}$$

with θ_W being the weak mixing angle. These Lagrangian terms can be described by the Feynman diagrams in figure 1.

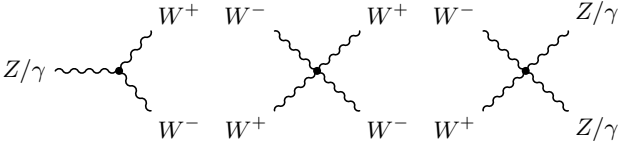


Figure 1: Feynman diagrams for SM gauge boson self-coupling contributions.

2.2 Effective Field Theories

In Fermi's theory of β -decay the decay of a neutron to a proton, an electron and an antineutrino is described by quartic couplings with coupling strength G_F while in the theory of weak interaction it is described by gauge boson exchange. Fermi's theory is only valid for much smaller energies than the W boson mass M_W while the theory of weak interaction is valid over the whole energy scale. Fermi's theory of β -decay is a so called "effective field theory" (EFT) simplifying the description of weak interaction for a low energy scale.

An effective field theory yields the possibility to describe new physics which is separated from the accessible region (\sim center-of-mass energy \sqrt{s}) by a different energy scale Λ ($s \ll \Lambda^2$). To establish an EFT

one builds a parametrized, most general Lagrangian fulfilling the process properties, which should recover the SM in the limit $\Lambda \rightarrow \infty$. In other words it should preserve Unitarity. Such an EFT yields a model independent approach for physics beyond the SM (BSM).

2.3 Effective Field Theory Approach for Triple and Quartic Gauge Couplings

Beyond the SM triple and quartic gauge couplings could arise from higher order contributions of new physics. To be able to include such contributions in the theoretical description one introduces EFTs describing the triple and quartic couplings in a general way.

2.3.1 Neutral Triple Gauge Couplings

Neutral triple gauge couplings (nTGC) are forbidden in the SM but could be realized as "anomalous"² coupling in an EFT approach. One constructs the EFT Lagrangian from the general process properties applying the following constraints:

- There are nine helicity states in total but only seven valid because of angular momentum conservation.
- Bose statistics have to be respected.

This yields the following ZZV^3 Lagrangian

$$\begin{aligned}
\mathcal{L}_{ZZV} = & \frac{e^2}{M_Z^2} \left(- [f_4^\gamma (\partial_\mu F^{\mu\nu}) + f_4^Z (\partial_\mu Z^{\mu\nu})] \right. \\
& \times Z_\sigma (\partial^\sigma Z_\nu) \\
& - [f_5^\gamma (\partial^\rho F_{\rho\lambda}) + f_5^Z (\partial^\rho Z_{\rho\lambda})] \\
& \left. \times \tilde{Z}^{\lambda\xi} Z_\xi \right), \quad (11)
\end{aligned}$$

where e is the elementary charge, M_Z is the Z mass, f_i^V are the couplings and the following definitions are used

$$Z_{\mu\nu} := \partial_\mu Z_\nu - \partial_\nu Z_\mu, \quad (12)$$

$$\tilde{Z}^{\mu\nu} := \frac{1}{2} \epsilon^{\mu\nu\alpha\beta} Z_{\alpha\beta}. \quad (13)$$

The couplings f_4^V belong to CP violating processes while the f_5^V belong to CP conserving ones.

For this Lagrangian possible contributions to the couplings are mentioned exemplary:

- *SM contributions:*
NLO and higher order contributions (only to CP conserving f_5^V)

²"Anomalous" meaning not realized in the SM.

³ V can either be γ or Z .

- *MSSM contributions:*
1-loop and higher order contributions from charginos and neutralinos
- *New boson contributions:*
CP violating coupling f_4^V sensitive to two-Higgs-doublet model in 1-loop corrections

2.3.2 Charged Triple Gauge Couplings

Charged triple gauge couplings (cTGC) are already realized as ZWW and γWW in the SM (see figure 1). Further contributions may arise from new physics BSM in an EFT approach. The EFT Lagrangian is constructed in a similar way as the nTGC following the constraint on helicity states and demanding additionally C and P conservation⁴. It is given by

$$\begin{aligned} \mathcal{L}_{WWV} = & ig_{WWV} \left(g_1^V (W_{\mu\nu}^+ W^{-\mu} - W^{+\mu} W_{\mu\nu}^-) V^\nu \right. \\ & + \kappa_V W_\mu^+ W_\nu^- V^{\mu\nu} \\ & \left. + \frac{\lambda_V}{M_W^2} V^{\mu\nu} W_\nu^{+\rho} W_{\rho\mu}^- \right) \end{aligned} \quad (14)$$

where $W_{\mu\nu}^\pm$ is the rank two tensor

$$W_{\mu\nu}^\pm := \partial_\mu W_\nu^\pm - \partial_\nu W_\mu^\pm, \quad (15)$$

g_1^V , κ^V and λ_V are the couplings, $g_{WW\gamma} = e$ and $g_{WWZ} = e \cot \theta_W$. Because of the electric charge of the W boson the relation

$$g_1^\gamma = 1 \quad (16)$$

holds. Taking only into account SM contributions the general cTGC couplings are given by

$$g_1^Z = \kappa_Z = \kappa_\gamma = 1, \quad (17)$$

$$\lambda_Z = \lambda_\gamma = 0. \quad (18)$$

Often the deviations from the SM

$$\Delta g_1^Z = g_1^Z - 1 \quad (19)$$

$$\Delta \kappa_Z = \kappa_Z - 1 \quad (20)$$

$$\Delta \kappa_\gamma = \kappa_\gamma - 1 \quad (21)$$

and not the absolute values are denoted.

2.3.3 Quartic Gauge Couplings

In the SM quartic gauge couplings (QGC) are realized as $WWWW$, $WWZZ$, $WW\gamma Z$ and $WW\gamma\gamma$ (see figure 1). Further contributions from BSM physics might be possible in an EFT approach. An EFT Lagrangian is constructed under the following constraints:

⁴Demanding C and P conservation is only a reasonable guess to reduce the degrees of freedom of the theory.

- Consider couplings to the longitudinal polarization degree of gauge bosons only.
- Custodial symmetry

$$\rho = \left(\frac{M_W}{M_Z \cos \theta_W} \right)^2 = 1 \quad (22)$$

should be respected.

Only vector boson scattering (VBS) terms in the Lagrangian are examined in this review. They are

$$\mathcal{L}_4 = \frac{\alpha_4}{16\pi^2} \text{Tr}(V_\mu V_\nu) \text{Tr}(V^\mu V^\nu), \quad (23)$$

$$\mathcal{L}_5 = \frac{\alpha_5}{16\pi^2} \text{Tr}(V_\mu V^\mu) \text{Tr}(V_\nu V^\nu), \quad (24)$$

where

$$V_\mu = -igW_\nu + ig'B_\mu \quad (25)$$

in unitary gauge and α_4 and α_5 are the couplings.

3 Limits on Anomalous Neutral Triple Gauge Couplings

The measurement of the ZZ production in pp collisions at the LHC yields a good possibility to determine nTGCs: Limits on anomalous ZZZ and $ZZ\gamma$ couplings can be well obtained from the differential cross section $\frac{d\sigma_{ZZ}}{dp_T^2}$. In the following some important techniques and results on nTGC from the ATLAS collaboration are presented. For a more detailed description please read [3].

Two different signal channels

- $ZZ^{(*)} \rightarrow l^+ l^- l^+ l^-$ and
- $ZZ \rightarrow l^+ l^- \nu \bar{\nu}$

were used. Their signal regions were defined by:

$ZZ^{(*)} \rightarrow 1^+ 1^- 1^+ 1^-$:

- exactly 4 isolated leptons, two same-flavour opposite charge pairs ($e^+ e^- e^+ e^-$, $e^+ e^- \mu^+ \mu^-$ or $\mu^+ \mu^- \mu^+ \mu^-$)
- $\Delta R(l_1, l_2) > 0.2^5$
- ambiguity in lepton combinations removed by choosing combination with lowest $|m_{l+l-} - M_Z|$
- at least one lepton pair fulfills $66 < m_{l+l-} < 116$ GeV (the other $m_{l+l-} > 20$ GeV)

$ZZ \rightarrow 1^+ 1^- \nu \bar{\nu}$:

- exactly 2 leptons of same flavour with $p_T > 20$ GeV
- $\Delta R(l_1, l_2) > 0.3$
- $76 < m_{l+l-} < 106$ GeV

⁵ $\Delta R = \sqrt{\Delta\phi^2 + \Delta\eta^2}$ is the geometrical distance of two objects separated by their azimuthal-angle-difference and pseudorapidity.

- axial- $E_T^{miss} = -\vec{E}_T^{miss} \cdot \vec{p}_T^Z / p_T^Z > 75$ GeV and $|E_T^{miss} - p_T^Z| / p_T^Z < 0.4$ to minimize Z +jet background (see figure 2 and 3)
- jet veto to mostly remove top-quark production background
- no additional lepton with $10 < p_T \leq 20$ GeV to reduce WZ background

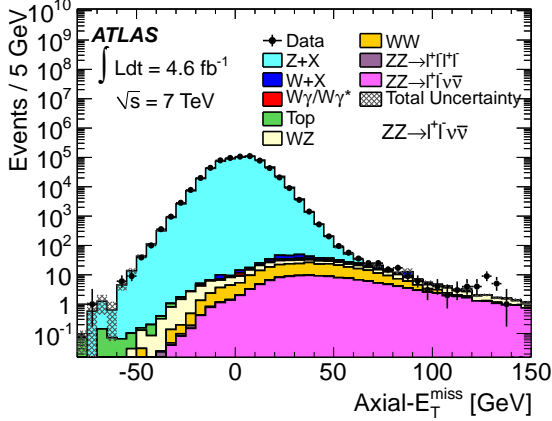


Figure 2: axial- E_T^{miss} distribution for data and predicted signal after all section requirements, except for cut axial- E_T^{miss} as presented in [3].

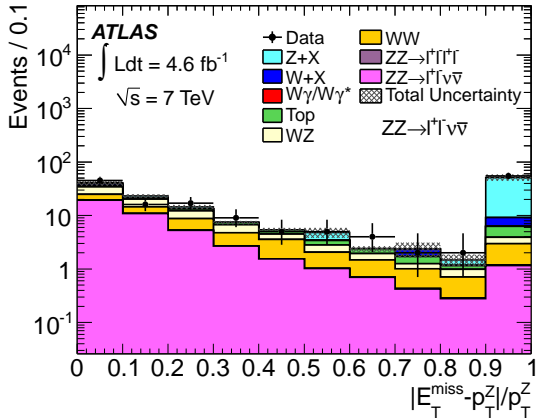


Figure 3: Fractional p_T difference distribution for data and predicted signal after all section requirements, except for cut on the fractional p_T difference as presented in [3].

3.1 Important Techniques Used in the $pp \rightarrow ZZ$ Analysis

3.1.1 Extended-Lepton Selection

To increase the selection acceptance in the $ZZ^{(*)} \rightarrow l^+l^-l^+l^-$ channel leptons which are normally dis-

carded due to detector geometry are used (= extended-leptons). Three categories of extended-leptons are defined in the given analysis and at most one lepton from each extended category is allowed to not increase the background. The extended-lepton categories are:

a) Forward spectrometer muons

Forward spectrometer muons are defined to be outside the nominal inner detector (ID) range with an allowed pseudorapidity range of $2.5 < |\eta| < 2.7$. They are required to *a)* a full track in the muon spectrometer, *b)* $p_T > 10$ GeV and *c)* $\sum E_T$ of calorimeter deposits inside of $\Delta R = 0.2$ smaller than 15% of muon p_T to remove fake muons from heavy flavoured hadron decay.

b) Calorimeter-tagged muons

Calorimeter-tagged muons are muons inside the muon spectrometer limited coverage range $|\eta| < 0.1$. They are required to *a)* have calorimeter deposit consistent with a muon which is matched to an ID track *b)* have $p_T > 20$ GeV and *c)* fulfill the same impact parameter and isolation criteria as “standard muons”. (See [3] for details.)

c) Calorimeter-only electrons

Calorimeter-only electrons lie outside the ID range with a pseudorapidity of $2.5 < |\eta| < 3.16$. They are required to *a)* have $p_T > 20$ GeV and *b)* pass the tight identification requirements. Their p_T is calculated from the calorimeter energy and electron direction. The charge is assigned depending on the charge of the other electron(s) in the event.

3.1.2 Data-Driven Background Estimation

The total background in the $ZZ \rightarrow l^+l^-l^+l^-$ channel $N(BG)$ is estimated via a data-driven method using

$$N(BG) = [N(lll_j) - N(ZZ)] \times f - N(ll_jj) \times f^2, \quad (26)$$

where

- $N(lll_j)$ is the number of events with 3 leptons and 1 lepton-like jet⁶ satisfying all selection criteria,
- $N(ll_jj)$ is the number of events with 2 leptons and 2 lepton-like jet satisfying all selection criteria,
- $N(ZZ)$ is a Monte-Carlo (MC) estimate for real leptons classified as lepton-like jet,

⁶A lepton-like jet is for example a muon candidate failing the isolation requirement or impact parameter requirement but not both.

- f is the ratio of the probability for a non-lepton to satisfy the full lepton selection criteria to the probability for a non-lepton to satisfy the lepton-like jet criteria.

The last summand in equation (26) removes double counting. The ratio f is derived from an independent sample containing one Z candidate (l^+l^-).

Part of the $ZZ \rightarrow l^+l^-\nu\bar{\nu}$ channel's background estimation is data-driven, too. The background resulting from $t\bar{t}$, Wt , WW and $Z \rightarrow \tau^+\tau^-$ events N_{ee}^{bkg} is estimated by

$$N_{ee}^{bkg} = (N_{e\mu}^{data} - N_{e\mu}^{sim}) \times \frac{1}{2} \times \frac{\epsilon_{ee}}{\epsilon_{e\mu}} \quad (27)$$

Here, $N_{e\mu}^{data}$ is the number of events in data when changing the same flavour lepton requirement to a different flavour lepton requirement (control sample) and $N_{e\mu}^{sim}$ is a MC estimate for non- $t\bar{t}$, $-Wt$, $-WW$ and $-Z \rightarrow \tau^+\tau^-$ events. Henceforth the first summand is an estimate for $t\bar{t}$, Wt , WW and $Z \rightarrow \tau^+\tau^-$ in the control sample. By using the correct branching fraction and efficiency ($\epsilon_{l\nu}$) corrections the background resulting from the given processes in the signal region is derived.

3.2 Obtaining Limits on Neutral Triple Gauge Couplings

To ensure that unitarity is not violated at LHC energies the couplings are parametrized in a form-factor approach meaning

$$f_i^V = \frac{1}{(1 + \hat{s}/\Lambda^2)^n} f_{i,0}^V \xrightarrow{s \rightarrow \infty} 0. \quad (28)$$

The form factor parameters are chosen to be $n = 3$ and $\Lambda = 3$ TeV. Simulated p_T^Z (transverse momentum of the leading Z boson) distributions for different f_i^V are generated using a matrix element amplitude reweighting method. From these the dependency of the couplings on the expected number of events in each p_T^Z bin is parametrized and limits are obtained using a maximum likelihood fit of the data.

3.3 Results on Limits on Neutral Triple Gauge Couplings

The limits on the couplings were obtained assuming all other couplings to be zero. The results supersede those from previous analyses and other colliders and are presented in table 1 and figure 4.

Table 1: One-dimensional 95% confidence intervals for anomalous neutral triple gauge couplings as presented in [3].

Λ	f_4^γ	f_4^Z	f_5^γ	f_5^Z
3 TeV	[-0.022, 0.023]	[-0.019, 0.019]	[-0.023, 0.023]	[-0.020, 0.019]
∞	[-0.015, 0.015]	[-0.013, 0.013]	[-0.016, 0.015]	[-0.013, 0.013]

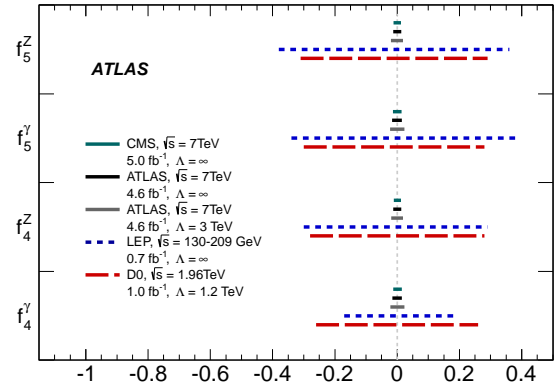


Figure 4: Comparison of one-dimensional 95% confidence intervals for anomalous neutral triple gauge couplings from different experiments as presented in [3].

4 Limits on Charged Triple Gauge Couplings

The measurement of WW production in pp collisions at the LHC provides a good possibility to test the electroweak sector of the SM and check for non-SM anomalous cTGC. In the following the results on limits on cTGC from the ATLAS collaboration and some techniques as presented in [4] are shown. Similar to section 3 the differential cross section $\frac{d\sigma_{WW}}{dp_T}$ is used to obtain limits on the couplings.

WW events are selected by their signature " $l'l' + E_T^{miss}$ ". The signal region selection criteria are

- two opposite charged leptons, where at least one is matched to a trigger reconstructed lepton (this results in 3 subchannels: ee , $e\mu$, $\mu\mu$),
- a cut on the invariant lepton mass $m_{l'l'}$ and $E_{T,Rel}^{miss}$, where

$$E_{T,Rel}^{miss} = \begin{cases} E_T^{miss} \times \sin(\Delta\phi) & \text{if } \Delta\phi < \pi/2 \\ E_T^{miss} & \text{if } \Delta\phi \geq \pi/2 \end{cases} \quad (29)$$

and $\Delta\phi$ is the azimuthal angle difference between E_T^{miss} and the nearest lepton or jet to remove most of the Drell-Yan background,

- a jet veto to diminish the $t\bar{t}$ and single top background and
- a cut on the two lepton system transverse momentum, $p_T(l'l') > 30$ GeV, to further reduce the Drell-Yan background.

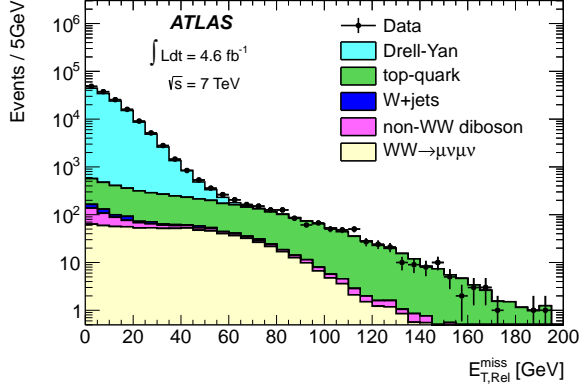


Figure 5: Data and predicted signal distribution of $E_{T,Rel}^{miss}$ before the $E_{T,Rel}^{miss}$ cut for the $\mu\mu$ subchannel as presented in [4].

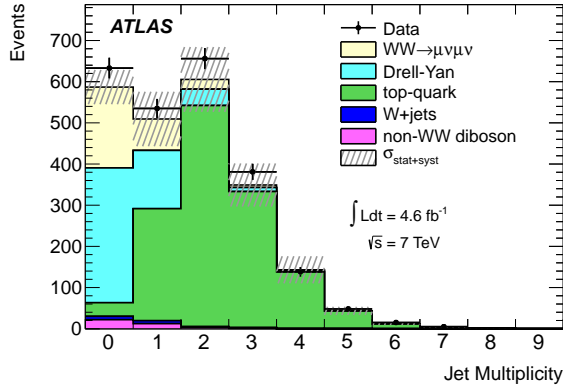


Figure 6: Data and predicted signal distribution of the jet multiplicity before the jet veto for the $\mu\mu$ subchannel as presented in [4].

4.1 Coupling Scenarios to Reduce Parameter Space

As the parameter space is too vast for the amount of data taken, three scenarios with different constraints on the couplings are assumed to be realized: In the “*equal coupling scenario*” γ and Z couplings are assumed to be the same

$$\Delta\kappa_Z = \Delta\kappa_\gamma, \lambda_Z = \lambda_\gamma \text{ and } g_1^Z = 1, \quad (30)$$

thus a total number of two free parameters is remaining.

The “*LEP scenario*”, used at the LEP experiment analyses [7], has three free parameters and is given by

$$\Delta\kappa_\gamma = \frac{\cos^2 \theta_W}{\sin^2 \theta_W} (\Delta g_1^Z - \Delta\kappa_Z) \text{ and } \lambda_Z = \lambda_\gamma. \quad (31)$$

The last scenario investigated is the “*HISZ scenario*” named after its inventors Hagiwara, Ishihara, Szalapski and Zeppenfeld with two free parameters [8]. It is motivated by $SU(2) \times U(1)$ invariance and described by

$$\Delta g_1^Z = \frac{1}{\cos^2 \theta_W - \sin^2 \theta_W} \Delta\kappa_Z, \quad (32)$$

$$\Delta\kappa_\gamma = 2\Delta\kappa_Z \frac{\cos^2 \theta_W}{\cos^2 \theta_W - \sin^2 \theta_W}, \quad (33)$$

$$\lambda_Z = \lambda_\gamma. \quad (34)$$

4.2 Results on Limits on Charged Triple Gauge Couplings

Limits were obtained in a similar manner to section 3.2 with form factor approach, reweighting method, determination of the dependency of the leading lepton transverse momentum $p_T(l_1)$ on the couplings and maximum likelihood fit. 95% confidence level limits were calculated for each of the three given scenarios and assuming that there is no relation between the couplings and that all other couplings except the one under study are zero. The results are presented in table 2, 6 and figure 7. They are more stringent than the results from the Tevatron experiments and in the same range as the LEP results.

Table 2: One-dimensional 95% confidence intervals for anomalous charged triple gauge couplings assuming all other than the one coupling investigated to be zero with form factor parameter $\Lambda = \infty$ as presented in [4].

Parameter	Expected	Observed
$\Delta\kappa_Z$	[-0.077,0.086]	[-0.078,0.092]
λ_Z	[-0.071,0.069]	[-0.074,0.073]
λ_γ	[-0.144,0.135]	[-0.152,0.146]
Δg_1^Z	[-0.449,0.546]	[-0.373,0.562]
$\Delta\kappa_\gamma$	[-0.128,0.176]	[-0.135,0.190]

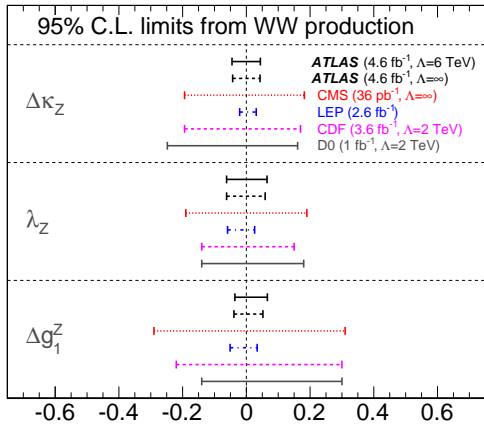


Figure 7: Comparison of one-dimensional 95% confidence intervals for anomalous charged triple gauge couplings in the LEP scenario from different experiments as presented in [4].

5 Electroweak $W^\pm W^\pm jj$ Production in pp Collisions and Limits on Quartic Gauge Couplings

After the discovery of the Higgs boson, which might unitarize vector boson scattering (VBS) amplitudes, the effort on searches for VBS has remarkably increased. One important final state from proton-proton collisions predicted to be showing VBS contributions is the two same-sign W bosons with two jets ($W^\pm W^\pm jj$) state. In the following the results from the ATLAS collaboration showing evidence for VBS on this final state and the results on limits on anomalous QGC are summarized. A more detailed description is given by [5].

The signal region was attempted to be enriched in electroweak production of $W^\pm W^\pm jj$, which is represented by weak interactions inclusively at Born level, and contain as less strong production $W^\pm W^\pm jj$, represented by both strong and weak interactions at Born level, as possible. (See figure 8.) It is defined by

- two same electric charge leptons,
- two jets with transverse momentum $p_T > 30$ GeV and pseudorapidity $|\eta| < 4.5$,
- an additional loose lepton veto to reduce $WZ/\gamma^* + X$ and $ZZ + X$ background,
- a cut on the invariant lepton mass $m_{ll} > 20$ GeV,
- the requirement of $|m_{ee} - M_Z| > 10$ GeV to re-

duce Z +jet background,

- a cut on the missing transverse energy $E_T^{miss} > 40$ GeV
- a b-jet veto to remove non-prompt electron background (mostly $t\bar{t} \rightarrow l\nu jj b\bar{b}$)
- a cut on the jet invariant mass $m_{jj} > 500$ GeV to further reduce $t\bar{t}$ and $WZ/\gamma^* + X$ background (see figure 9) and
- a requirement on the jet rapidity difference $|\Delta y_{jj}| > 2.4$ (see figure 10).

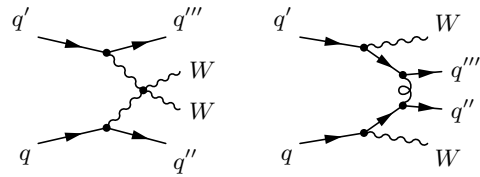


Figure 8: Showcase Feynman diagrams for electroweak $W^\pm W^\pm jj$ production (left diagram) and strong $W^\pm W^\pm jj$ production (right diagram).

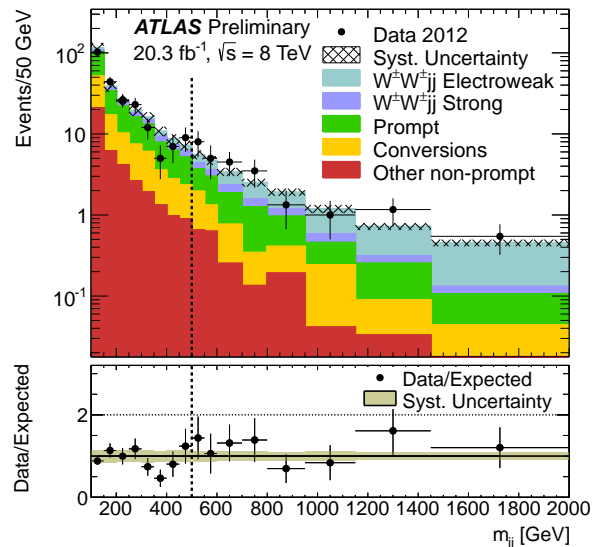


Figure 9: m_{jj} distribution for data and predicted signal after all selection requirements except the cut on m_{jj} as presented in [5].

5.1 Results on Cross Section and Limits

The measured cross section in the signal region with statistic and systematic errors (in this ordering) is measured to be

$$\sigma = 1.3 \pm 0.4 \pm 0.2 \text{ fb}, \quad (35)$$

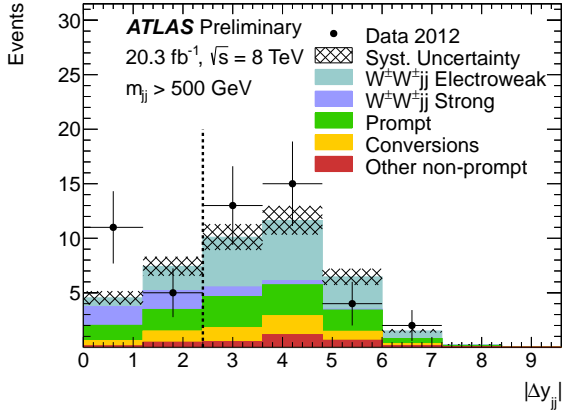


Figure 10: Δy_{jj} distribution for data and predicted signal after all selection requirements except the cut on Δy_{jj} as presented in [5]

which is in good agreement with the SM expectations of

$$\sigma = 0.95 \pm 0.06 \text{ fb}, \quad (36)$$

yielding an observation significance of 3.6 for electroweak production.

The total cross section is also used to set limits on anomalous QGC. The expected and observed 95% confidence limits are derived via a maximum likelihood fit. They are presented in figure 11.

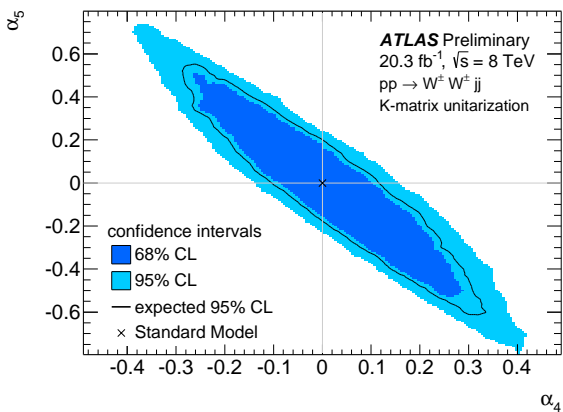


Figure 11: 95% and 68% confidence limits on QGC couplings α_4 and α_5 calculated from $W^\pm W^\pm jj$ cross section as presented in [5].

6 Future Results on Quartic Gauge Couplings

As triboson production and VBS are directly sensitive to QGC a detailed investigation might give deeper insights into the electroweak sector of SM and lead to discovery of new physics. Current analyses have not enough data at their disposal but the Phase 2 upgrade of the ATLAS detector and future LHC runs with high luminosity will increase the sensitivity in the important regions. In the following, some studies on future results at the ATLAS experiment on QGC are presented. For a more detailed description please follow [6].

The effects of five $SU(2)_L \times U(1)$ gauge-invariant, CP conserving operators are investigated. Their couplings are

- $c_{\phi W}/\Lambda^2$, associated with a dimension-6 operator and affected by triboson production and VBS but not diboson production,
- f_{s0}/Λ^4 , associated with a dimension-8 operator, related to α_4 (see equation (23) and section 5),
- $f_{T_{1/8/9}}/\Lambda^4$, set of couplings associated with dimension-8 operators not directly affecting the Higgs boson couplings.

Neither of the couplings is affected by the constraints on TGC from old analyses or the above mentioned. Each of the couplings can be well examined by special processes for which their impact to the final state is quite high.

6.1 Future Vector Boson Scattering Analysis Using the $ZZ \rightarrow lljj$ Final State

The final state $ZZ \rightarrow lljj$ is sensitive to the coupling $c_{\phi W}/\Lambda^2$, perfectly triggerable and very well reconstructable. Assuming that the background is composed of SM ZZ production only, which was shown to be perfectly reasonable (see [9]), the 5σ discovery potentials are given by table 3.

Table 3: 5σ -significance discovery values of $c_{\phi W}/\Lambda^2$ for different integrated luminosities at a center of mass energy $\sqrt{s} = 14 \text{ TeV}$ as presented in [6].

	300 fb ⁻¹	3000 fb ⁻¹
$c_{\phi W}/\Lambda^2$	34 TeV ⁻²	16 TeV ⁻²

6.2 Future Vector Boson Scattering Analysis Using the $WZ \rightarrow l\nu ll$ Final State

The final state $WZ \rightarrow l\nu lljj$ is sensitive to the coupling f_{T1}/Λ^4 and can be quite well reconstructed by using the W boson mass constraint. Assuming that the background is composed of SM WZ production only, the 5σ discovery potentials are given in table 4.

Table 4: 5σ -significance discovery values of f_{T1}/Λ^4 for different integrated luminosities at a center of mass energy $\sqrt{s} = 14$ TeV as presented in [6].

	300 fb ⁻¹	3000 fb ⁻¹
f_{T1}/Λ^2	1.3 TeV ⁻⁴	0.6 TeV ⁻⁴

6.3 Future Triboson Production Analysis Using the $Z\gamma\gamma$ Final State

The final state $Z\gamma\gamma$ is sensitive to BSM triboson production and the couplings f_{T8}/Λ^4 and f_{T9}/Λ^4 can be determined by this final state. It is well reconstructable in case of leptonic decay of the Z boson. The event selection criteria are:

- $p_T(l) > 25$ GeV
- $|\eta(l)| < 2.0$
- $p_T(\gamma) > 25$ GeV
- $|\eta(\gamma)| < 2.0$
- At least one lepton and one γ with $p_T > 160$ GeV, improving the sensitivity of anomalous QGC
- $|m_{ll} - 91 \text{ GeV}| < 10 \text{ GeV}$, to suppress γ^* contributions to the dilepton
- $\Delta(\gamma, \gamma) > 0.4$, $\Delta(l, \gamma) > 0.4$, $\Delta(l, l) > 0.4$, to reduce final state radiation contributions.

Assuming that the background is composed of SM $Z\gamma j$ and Zjj , the 5σ discovery potentials are given in table 5.

Table 5: 5σ -significance discovery values of f_{T8}/Λ^4 and f_{T9}/Λ^4 for different integrated luminosities at a center of mass energy $\sqrt{s} = 14$ TeV as presented in [6].

	300 fb ⁻¹	3000 fb ⁻¹
f_{T8}/Λ^2	0.9 TeV ⁻⁴	0.4 TeV ⁻⁴
f_{T9}/Λ^2	2.0 TeV ⁻⁴	0.7 TeV ⁻⁴

7 Conclusion

Hadron collider final states with two gauge bosons yield great opportunities to measure and investigate multiple gauge boson couplings. Triple and quartic gauge couplings can be well described in an effective field theory approach yielding the possibility to not only test the electroweak sector of the SM but also probe for new physics BSM in a model independent way. Results from three analyses from the ATLAS experiment at the LHC were presented in this article. They could improve the limits on anomalous nTGC from LEP [3] and reach a similar precision on limits on cTGC [4]. Additionally evidence for electroweak production of $W^\pm W^\pm jj$ was shown which gives first direct constraints on anomalous QGC. No physics BSM could be observed but it might be hidden due to low precision which can be improved by run 2 of the LHC. A study on future prospects indicates that triboson production and further VBS analyses yielding limits on anomalous QGC may be realizable for the new phase and might give quite precise results after enough data being collected.

References

- [1] S. Rosati. Study of triple and quartic gauge boson couplings in e^+e^- collisions between 180 and 800 GeV. *Dissertation, Bonn*, 2002.
- [2] H. Voss. Measurement of the triple gauge boson couplings in W -pair production with OPAL. *Dissertation, Bonn*, 2000.
- [3] ATLAS collaboration. Measurement of ZZ production in pp collisions at $\sqrt{s}=7$ TeV and limits on anomalous ZZZ and $ZZ\gamma$ couplings with the ATLAS detector. *Journal of High Energy Physics*, 2013(3):128, 2013.
- [4] ATLAS collaboration. Measurement of W^+W^- production in pp collisions at $\sqrt{s}=7$ TeV with the ATLAS detector and limits on anomalous WWZ and $WW\gamma$ couplings. *Phys.Rev.*, D87(11):112001, 2013.
- [5] ATLAS collaboration. Evidence for electroweak production of $W^\pm W^\pm jj$ in pp collisions at $\sqrt{s} = 8$ TeV with the ATLAS detector. Technical Report ATLAS-CONF-2014-013, CERN, Geneva, March 2014.
- [6] ATLAS collaboration. Studies of Vector Boson Scattering And Triboson Production with an Upgraded ATLAS Detector at a High-Luminosity

LHC. Technical Report ATL-PHYS-PUB-2013-006, CERN, Geneva, June 2013.

- [7] G. Gounaris, J.L. Kneur, D. Zeppenfeld, Z. Ajaltouni, A. Arhrib, et al. Triple gauge boson couplings. 1996.
- [8] K. Hagiwara, S. Ishihara, R. Szalapski, and D. Zeppenfeld. Low energy effects of new interactions in the electroweak boson sector. *Phys. Rev. D*, 48:2182–2203, September 1993.
- [9] ATLAS collaboration. Measurement of the total ZZ production cross section in proton-proton collisions at $\sqrt{s} = 8$ TeV in 20 fb^{-1} with the ATLAS detector. Technical Report ATLAS-CONF-2013-020, CERN, Geneva, March 2013.

Table 6: One-dimensional 95% expected and observed limits for anomalous charged triple gauge couplings in the LEP, HISZ and Equal Couplings scenario assuming all other than the one coupling investigated to be zero as presented in [4].

Scenario	Parameter	Expected ($\Lambda = 6 \text{ TeV}$)	Observed ($\Lambda = 6 \text{ TeV}$)	Expected ($\Lambda = \infty$)	Observed ($\Lambda = \infty$)
LEP	$\Delta\kappa_Z$	[-0.043, 0.040]	[-0.045, 0.044]	[-0.039, 0.039]	[-0.043, 0.043]
	$\lambda_Z = \lambda_\gamma$	[-0.060, 0.062]	[-0.062, 0.065]	[-0.060, 0.056]	[-0.062, 0.059]
	Δg_1^Z	[-0.034, 0.062]	[-0.036, 0.066]	[-0.038, 0.047]	[-0.039, 0.052]
HISZ	$\Delta\kappa_Z$	[-0.040, 0.054]	[-0.039, 0.057]	[-0.037, 0.054]	[-0.036, 0.057]
	$\lambda_Z = \lambda_\gamma$	[-0.064, 0.062]	[-0.066, 0.065]	[-0.061, 0.060]	[-0.063, 0.063]
Equal Couplings	$\Delta\kappa_Z$	[-0.058, 0.089]	[-0.061, 0.093]	[-0.057, 0.080]	[-0.061, 0.083]
	$\lambda_Z = \lambda_\gamma$	[-0.060, 0.062]	[-0.062, 0.065]	[-0.060, 0.056]	[-0.062, 0.059]